Received: 15 May 2021 | Revised: 9 July 2021 | Accepted: 10 July 2021

DOI: 10.1002/jcla.23916

RESEARCH ARTICLE

WILEY

Microarray analysis of circRNAs sequencing profile in exosomes derived from bone marrow mesenchymal stem cells in postmenopausal osteoporosis patients

Miao Fu | Liping Fang | Xi Xiang | Xijing Fan | Junqi Wu | Jinhua Wang

Affiliated Jinhua Hospital, Zhejiang University School of Medicine, Jinhua, China

Correspondence
Junqi Wu and Jinhua Wang, Affiliated Jinhua Hospital, Zhejiang University School of Medicine, Jinhua 321000, Zhejiang, China.
Emails: jhwujunqi@sina.com (JWu); 4470000@qq.com (JW)

Funding information
This work was supported by the grants from the Scientific Research Fund Project of the Science and Technology Program of traditional Chinese Medicine in Zhejiang Province (No. 2021ZA142), Jinhua Science and Technology Plan Project Commonweal Project (No. 2018-4-040), Health Science and Technology Project of Zhejiang Province (No. 2021KY1180), and Start-up Fund for Young and Middle-aged Scientific Research in Jinhua Central Hospital (No. JY2017-2-11 and JY2019-2-08). Special scientific research project for emergency prevention and control of pneumonia of new coronavirus infections in Jinhua City (No. 2020XG-02). Public Welfare Fund Research Project of Zhejiang Province (No. LGD19C040004-1)

Abstract

Introduction: Bone marrow-derived mesenchymal stem cells (BMSCs)-derived exosomes are involved in the modulation of tissue repair and regeneration. CircRNAs play important roles in BMSCs exosomes. The current study sought to explore the role of circRNAs in exosomes derived from BMSCs of postmenopausal osteoporosis (PMOP) patients and the underlying mechanisms.

Methods: RNA was extracted from BMSCs exosomes of PMOP and a control group. RNA microarray and bioinformatics analyses were used to explore the expression profile and functions circRNAs. Differentially expressed circRNAs from 20 PMOP and 20 controls were analyzed using RT-qPCR.

Results: A total of 237 upregulated and 279 downregulated circRNAs were identified in the current study. The top-10 most upregulated circRNAs in the PMOP group were hsa_circ_0069691, hsa_circ_0005678, hsa_circ_0006464, hsa_circ_0015813, hsa_circ_0000511, hsa_circ_0076527, hsa_circ_0009127, hsa_circ_0047285, hsa_circ_0027741, and hsa_circ_0090949. The top-10 most downregulated circRNAs were hsa_circ_0048669, hsa_circ_0090247, hsa_circ_0070899, hsa_circ_0087557, hsa_circ_0045963, hsa_circ_0090180, hsa_circ_0058392, hsa_circ_0040751, hsa_circ_0067910, and hsa_circ_0049484. RT-PCR verified dysregulation of 5 circRNAs including hsa_circ_0009127, hsa_circ_0090759, hsa_circ_0058392, hsa_circ_0090247, and hsa_circ_0049484. Moreover, a circRNA-microRNA-mRNA interaction network was developed based on differentially expressed circRNAs. Functional analysis showed that pathways involved in the regulation of autophagy, PI3K-Akt signaling, FoxO signaling, and MAPK signaling were associated with the differentially expressed circRNAs in PMOP patients.

Conclusion: The findings of this study show dysregulated circRNAs in BMSCs exosomes of PMOP patients, which may affect the progression of PMOP. These circRNAs can be used as predictive biomarkers and as therapeutic targets for the treatment of PMOP.

Junqi Wu and Jinhua Wang, contributed equally to this work and should be considered as co- corresponding authors

KEYWORDS
bone marrow mesenchymal stem cells, circular RNA, exosome, postmenopausal osteoporosis

1 | INTRODUCTION

Postmenopausal osteoporosis (PMOP) is a systemic metabolic bone disease caused by a decrease in estrogen secretion and imbalance of bone resorption and bone formation in postmenopausal women.[1] Osteoporotic fractures, including hip fractures and vertebral compression fractures (VCFs), are the most severe manifestations of osteoporosis in elderly women, and the treatment may require high-risk surgery.[2] Previous studies report that higher programmed cell death protein 1 (PD-1) and systemic immune-inflammation index (SII) in the peripheral blood of PMOP patients have potential diagnostic application for PMOP.[3,4] Although sensitive and effective biomarkers have been identified for early identification of PMOP, current treatment strategies do not fully reverse osteoporosis. Bone marrow-derived mesenchymal stem cells (BMSCs) promoted bone regeneration and play important roles in maintaining normal bone metabolism.[5] Osteogenic differentiation defect is a major cause of osteoporosis. Transplanted exogenous MSCs reverse osteoporosis by regulating osteogenic differentiation of host MSCs,[6,7] although the underlying mechanism is not fully known.

Notably, communication between osteoblasts and osteoclasts takes place through small membrane-enclosed vesicular particles named as exosomes, which can fuse with the surrounding cell membranes within circulatory pathways.[8] Exosomes are membrane-bound vesicles whose diameter ranges from 40 to 200 nm and are secreted by various cells to mediate cell-cell communication.[9] Exosomes transfer bioactive lipids, nucleic acids, and proteins across cells.[10] Recent studies report that BMSCs-derived exosomes modulate bone metabolism and the bone microenvironment.[11,12] Efficient bone regeneration is mainly associated with the paracrine delivery of specific substances to receiving cells through exosomes. In vitro and in vivo studies report that BMSCs-derived exosomes protect cartilage from degeneration.[13,14] Exosomes produced by human-induced pluripotent stem cell-originated MSCs increase bone rejuvenation of critical-sized calvarial defects in ovariectomized rats by promoting osteogenesis and angiogenesis.[15] Furthermore, exosomes derived from BMSCs are more stable under diverse physiological conditions compared with stem cells and lack immunogenicity; thus, they are suitable for therapeutic intervention.[16] Therefore, exosomes derived from BMSCs are a promising treatment strategy for metabolic bone diseases, including PMOP.

Li et al.[17] reported that circular RNAs (circRNAs) are highly expressed in exosomes. CircRNAs can be divided into non-coding circRNAs and coding circRNAs based on ability to be translated.[18] Studies report that circRNAs act as competing endogenous RNAs (ceRNAs) by sponging miRNAs, thus counteracting their inhibitory effects on gene expression.[19,20] For example, circSERPINE2 plays a protective role in osteoarthritis by interacting with miR-1271 to regulate E26 transformation-specific-related gene (ERG) expression.[21] CircFOXP1 regulates MSC differentiation by interacting with miR-17-3p/miR-127-5p, and in vivo animal experiments show that circFOXP1 modulates MSC bone repair.[22] These studies indicate that circRNA modulates growth, regeneration, and function of osteoblasts, chondrocytes, and osteoclasts. However, the expression profile and mechanism of circRNAs in BMSCs exosomes during PMOP have not been explored.

In the current study, the circRNA expression profile in BMSCs exosomes from PMOP patients was explored through microarray analysis and was compared with that of controls to identify differentially expressed circRNA. Sequence annotation and functional analysis were performed to elucidate the putative biological functions of genes targeted by the differential circRNA candidates. The findings showed that differentially expressed circRNAs are implicated in the modulation of PMOP pathogenesis through autophagy, AMPK signaling, and PI3K-Akt signaling. These findings provide important information for guiding further research on diverse genes and cascades, which are implicated in the onset and progression of PMOP.

2 | MATERIALS AND METHODS

2.1 | Ethical statement

Ethical approval for the study was obtained from the ethics committee of Jinhua central hospital. All patients in included in the study signed an informed consent form.

2.2 | Patients and BMSCs isolation and culture

Patients treated for femoral head necrosis or femoral neck fracture at the department of joint surgery of Jinhua central hospital from March 2019 to June 2020 were included in this study. BMSCs were obtained by isolation and culture of the mixture of bone marrow and blood drawn from the femoral marrow cavity during total hip arthroplasty. Forty patients were selected for BMSCs isolation and culture. Out of the 40 patients, 20 were diagnosed with PMOP, and 20 were healthy controls. Osteoporosis was defined by spine or hip BMD (bone mineral density) T-score ≤-2.5 SD. Healthy controls were defined by spine or BMD T-score ≥-1.0 SD. Detailed participant characteristics are presented in Table S1. Samples were collected from patients during diagnosis or recurrence after obtaining written informed consent. Inclusion criteria included as follows: (a) no bone tumor or tumor-like lesions, (b) not under medication affecting bone metabolism (such as antacids containing aluminum, corticosteroids, antituberculosis drugs, heparin, and antiepileptic drugs), (c) no systemic disease affecting bone metabolism (such as deformans osteitis, hyperparathyroidism, osteochondrosis, osteogenesis imperfecta,

renal osteodystrophy, and diabetes hypoparathyroidism), and (d) no blood system disorders. BMSCs were isolated using the adherence technique in a special medium. The mix medium was flushed 36–48 h postinoculation to isolate MSCs from the marrow mixture. Primary cells were used in expression analysis after 3 passages and cultured in a growth medium for human BMSCs (Cyagen Biosciences) supplemented with 10% FBS, 1% L-glutamic acid, and 1% double antibiotics. BMSCs were cultured at 37°C under 5% CO^2.

2.3 | BMSCs characterization

Bone marrow-derived mesenchymal stem cells were characterized by the detection of cell surface antigens with flow cytometry. Passage 5 BMSCs (90% confluence) were rinsed in PBS 1X and detached using 2 ml 0.25% trypsin, for 4 min at 37°C. Cells were then resuspended in complete media, transferred into a microfuge tube, and centrifuged for 5 min at 100 *g*. The cell pellet was then rinsed twice with PBS 1X and centrifuged. After counting, cells were diluted to 1×10^5 cells/ml, centrifuged at 100 *g* for 5 min, and then resuspended in 200–200 μl PBS. The cell suspension was then stained with anti-CD90-APC, anti-CD44-FITC, anti-CD34-PE, and anti-CD45-PerCP/Cy5.5 for 20 min, under dark condition. The cell suspension was rinsed with 2 ml PBS 1X, centrifuged at 100 *g* for 5 min, and res-suspended in 200 μl buffer solution; then, flow cytometry (BD Biosciences) analysis was performed.

2.4 | Osteogenic differentiation of BMSCs

Passage 5 BMSCs were seeded on 24-well plates and cultured with osteogenic medium (Cyagen Biosciences) for 14 days. BMSCs were stained with 10% alizarin red dyestuff (Yeasen) for 10 min and rinsed thrice with PBS 1X followed by examination under an optical microscope (Olympus), and images were obtained.

2.5 | Adipogenic differentiation of BMSCs

Passage 5 BMSCs were inoculated in 24-well plates and grown in adipogenic differentiation basal medium A (Cyagen Biosciences). The medium was replaced with adipogenic differentiation basal medium B (Cyagen Biosciences) after 3 days, and cells grown for one more day. These steps were repeated up to day 14 (referred as the 3rd cycle). Cells were then fixed with 4% formalin solution and stained with Oil Red O (Yeasen) for 40 min followed by microscopic examination (Olympus).

2.6 | Isolation and identification of exosomes

Passage 3–6 BMSCs were inoculated in the growth medium for human BMSCs enriched with 10% FBS-free of exosomes and 1% pen/strep for 72 h. The growth medium was then collected and centrifuged at 200 *g* for 15 min to remove residual cells. A cell culture media exosome purification kit (Norgen, Canada) was used to isolate exosomes following manufacturer's instructions. Exosome surface biomarker proteins including CD81, CD63, and CD9 were explored by Western blotting and exosome ultrastructure was visualized by transmission electron microscopy (HT7700, Hitachi).

2.7 | Western blot

Exosomes and cells were lysed using RIPA buffer (Beyotime) centrifuged at 10,000 g for 20 min. BCA assay kit (Beyotime) was used to quantify the proteins. Proteins were separated on a 10% SDS-PAGE and subsequently blotted onto PVDF membranes. 5% skimmed milk was used to block the membranes for 1 h at room temperature (RT). The membranes were then incubated overnight with rabbit primary antibodies against CD63, β-actin, CD9, and CD81 (Abcam). Membranes were then washed thrice with TBST (Beyotime) and incubated with HRP-labelled goat anti-rabbit secondary antibody (Beyotime) for 1 h. Enhanced chemiluminescence (ECL) fluorescent detection kit (Beyotime) was used to tag samples with a fluorescence probe, and then, images were obtained using a gel imager. Protein band intensity was quantified by normalizing it based on β-actin band intensity.

2.8 | CircRNA microarray assay

An exosome RNA isolation kit (Norgen, Canada) was used to isolate total RNA from exosomes, and NanoDrop ND-2000 (Thermo Scientific) was used to quantify RNA. CircRNA microarray analysis (LC Biotech) was performed to identify differentially expressed circRNAs between PMOP ($n = 3$) and control ($n = 3$) samples. Strand-specific cDNA libraries were processed as described previously.[23] Processing of raw reads was performed through the removal of adaptor reads along with low-quality tags. Clean reads were used in downstream analyses. Agilent Scanner G5761A (Agilent Technologies) was used to scan the original image post rolling hybridization at 65°C for 17 h. Raw data were normalized by quantile algorithm.

2.9 | Bioinformatics analysis

circRNAs gene symbols were submitted DAVID webserver, and KEGG pathway enrichment analyses were performed to explore the potential function of circRNAs. Genes and involved pathways were imported into Cytoscape 3.7.2 to construct a network to explore the biological functions of the circRNAs.

2.10 | RT-qPCR

One milligram of total RNA was used for first-strand cDNA synthesis using TransScript First-Strand cDNA synthesis kit (DF Biotech) according to manufacturer instructions. RT-qPCR was performed using SYBR green qPCR mix (DF Biotech) on a qTOWER2.2 Real-Time PCR system

(Analytik Jena AG, D-07745). For PCR analysis, 1 μl of cDNA and 0.5 μl of genomic DNA were used with 200 nM of convergent primers in a 25 μL reaction mix under the following cycling conditions: 95°C for 10 min, 40 cycles of 95°C for 15 s, and 60°C for 1 min. GAPDH was used as the internal control. The relative expression level was determined using the $2^{-\Delta\Delta Ct}$ method. Primer sequences used are shown in Table S2. The experiment was performed in triplicates.

2.11 | Statistical analyses

Statistical analyses were performed using SPSS program. Data were expressed as mean ± SD. Student's *t* test was used to compare differences between the 2 groups. $p < 0.05$ was considered statistically significant.

3 | RESULTS

3.1 | Phenotype identification of BMSCs

Bone marrow-derived mesenchymal stem cells were isolated using the direct adherent method. Primary BMSCs from healthy women and PMOP patients were cultured successfully. Analysis of BMSCs showed the presence of fibroblasts with high cell density, spindle-shape, and wall-attached edges (Figure 1A). Flow cytometry analysis of specific surface biomarkers (CD44 and CD90) and a hematopoietic biomarker (CD34 and CD45) in BMSCs showed CD44 and CD90 positive rates of 93.9% ± 1.83% and 99.7% ± 2.78%, respectively, and CD34 and CD45 positive rate at 4.3% ± 0.27% and 2.2% ± 0.25%, respectively (Figure 1B). Cells were positive for Oil

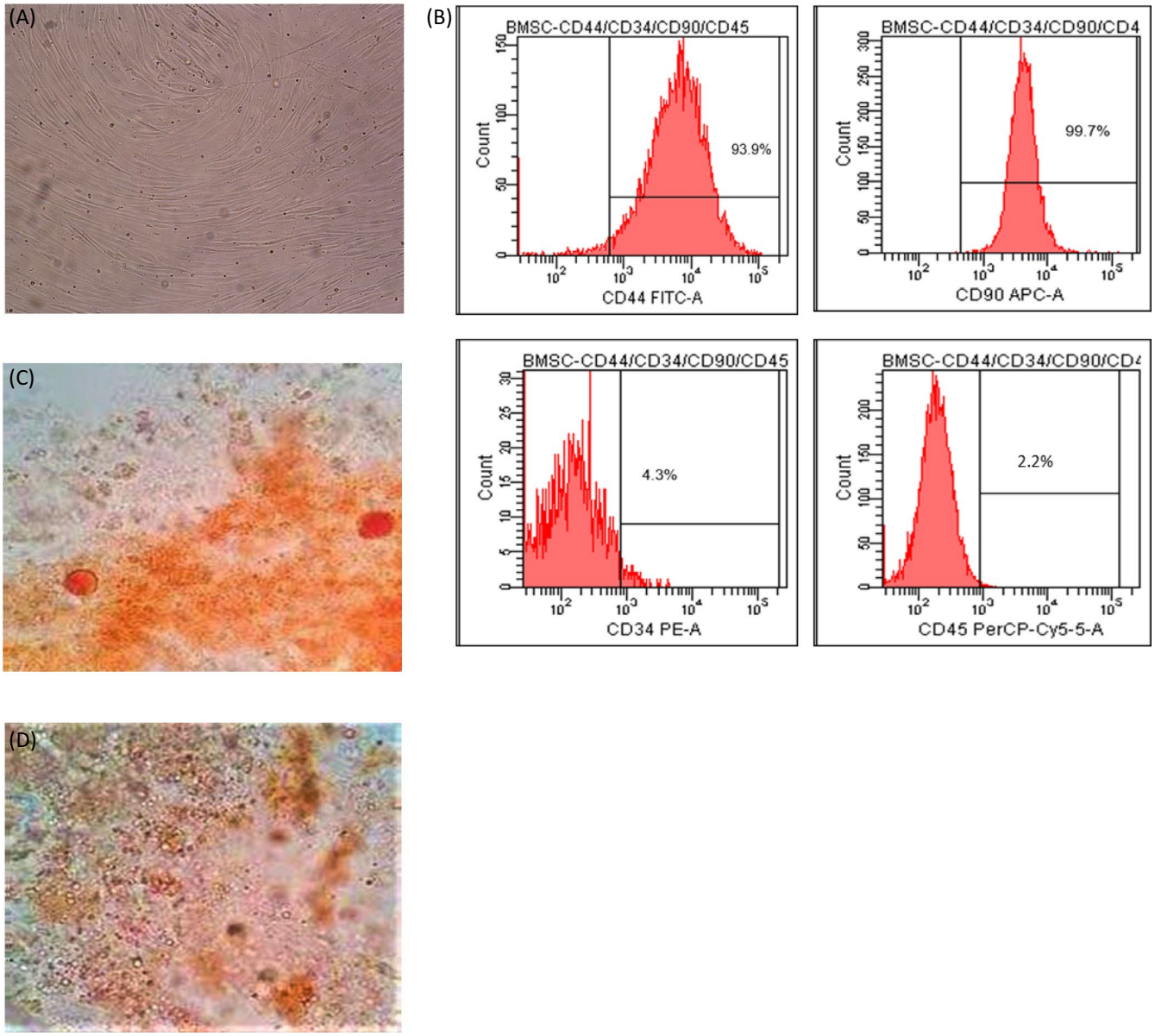

FIGURE 1 Characterization of BMSCs. (A) Primary BMSCs show spindle-shaped morphology. (B) Levels of BMSCs specific surface biomarkers (CD44 and CD90) and a hematopoietic biomarker (CD34 and CD45) as determined by flow cytometry. (C) Adipocytes stained with Oil Red O staining. (D) Mineralized nodules stained with alizarin red staining

Red O and alizarin red staining (Figure 1C,D), indicating adipogenic, and osteogenic differentiation of BMSCs. These findings show that the cells had the canonical phenotype and functional features of BMSCs.

3.2 | Identification of BMSCs-derived exosomes

Electron microscopy showed that BMSCs-derived exosomes had a 30–100 nm diameter (Figure 2A). Western blotting analysis of exosome proteins showed the presence of CD9, CD63, and CD81 (Figure 2B), implying that the isolated exosomes were similar to standard and could be used for subsequent experiments.

3.3 | Differential analysis of circRNAs in BMSCs-originated exosomes between PMOP group and control group

circRNA expression profiles were comparatively explored in the two exosome groups (Figure 3A). circRNA was considered to be differentially expressed if its level in the 2 groups differed by at least 1.5-fold ($p = <0.05$). Based on a normalized number of reads in the 2 groups, 237 upregulated and 279 downregulated circRNAs were identified between the PMOP BMSCs-derived exosomes and control BMSCs-derived exosomes (Figure 3B). The top-10 most upregulated circRNAs in the PMOP group included as follows: has_circ_0069691, hsa_circ_0005678, hsa_circ_0006464,

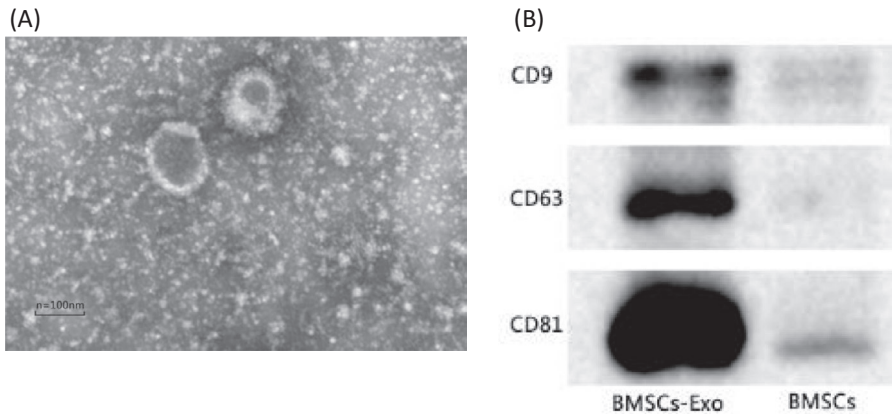

FIGURE 2 Characterization of BMSCs-derived exosomes. (A) Transmission electron microscopy characterization of BMSCs-derived exosomes. (B) Western blotting analysis of expression level of exosomal biomarker proteins CD9, CD63, and CD81

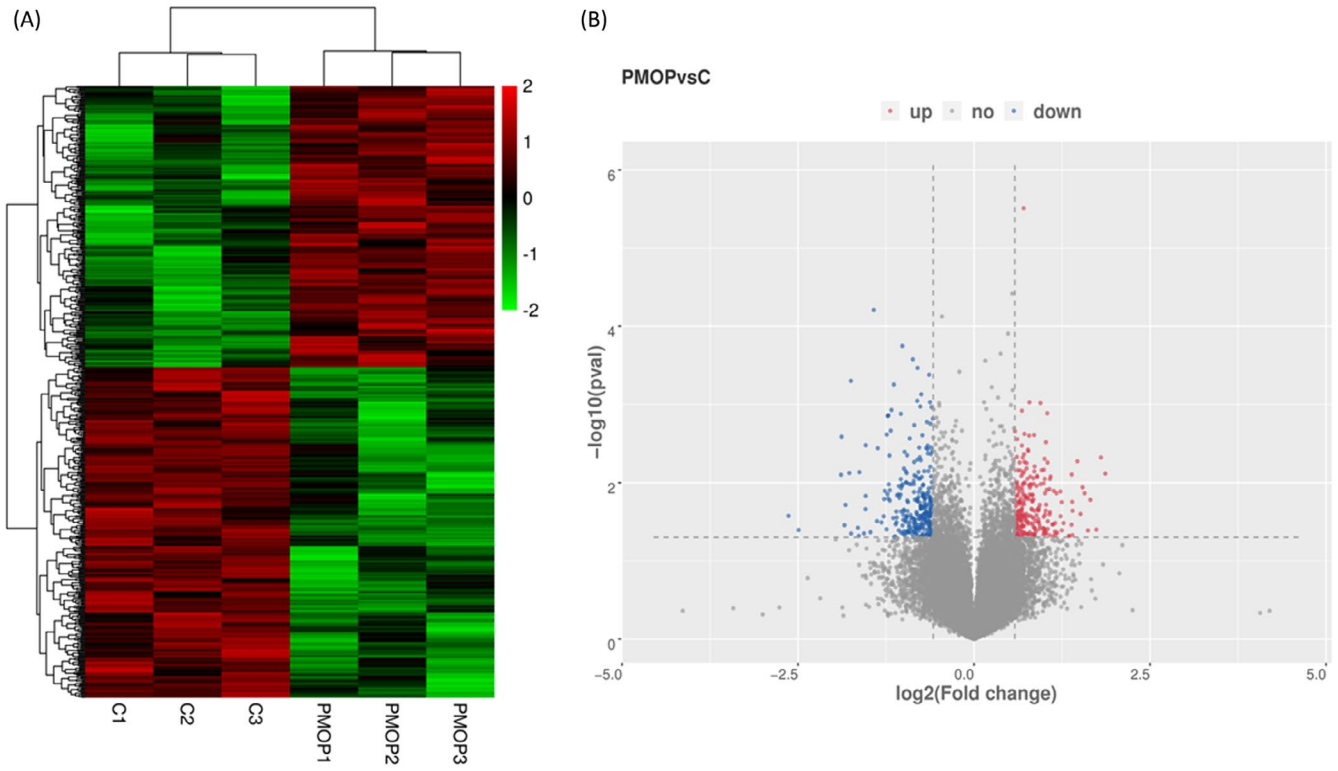

FIGURE 3 circRNAs expression patterns. (A) Cluster analysis of differentially expressed circRNAs. (B) Volcano plots showing relative expression in the two groups. Vertical lines represent 1.5-fold (log2 scaled) up and down, respectively. Horizontal lines represent *p*-value = 0.05 (-log10 scaled)

hsa_circ_0015813, hsa_circ_0000511, hsa_circ_0076527, hsa_circ_0009127, hsa_circ_0047285, hsa_circ_0027741, ahashsa_circ_0090949. Ton the hand, the top-10 most down-regulated circRNAs were hsa_circ_0048669, hsa_circ_0090247, hsa_circ_0070899, hsa_circ_0087557, hsa_circ_0045963, hsa_circ_0090180, hsa_circ_0058392, hsa_circ_0040751, hsa_circ_0067910, and hsa_circ_0049484 (Table S3).

3.4 | Validation of differentially expressed circRNAs by RT-qPCR

To validate RNA-seq results, 8 circRNAs ($p = <0.05$, fold change ≥2) and initial expression quantity were selected for RT-qPCR validation. The 8 circRNAs included 1 upregulated circRNA (hsa_circ_0009127,) and 7 downregulated circRNAs including hsa_circ_0090759, hsa_circ_0038264, hsa_circ_0058392, hsa_circ_0090247, hsa_circ_0049484, hsa_circ_0067910, and hsa_circ_0034487. To determine the expression levels of these circRNAs in BMSCs-originated exosomes, 40 samples were selected for validation (PMOP: $n = 20$ and Control: $n = 20$). The expression profiles for the 8 circRNAs were consistent with the microarray findings (Figure 4). Moreover, the expression profile of hsa_circ_0009127, hsa_circ_0090759, hsa_circ_0058392, hsa_circ_0090247, and hsa_circ_0049484 were significantly different between the two groups ($p < 0.01$, Figure 4).

3.5 | circRNAs functions as ceRNAs

MiRanda and Targetscan tools were used to explore the relationship between circRNAs-miRNAs-mRNAs, and intersection of the 2 software was used as interaction relationship among the 3 types of RNA. A network of circRNAs-miRNAs-mRNAs with 43 circRNAs, 23 miRNAs, and 65 mRNAs was developed by merging the common targeted miRNAs (Additional file 1). The enormous network information is challenging to display; therefore, circRNAs validated by RT-qPCR were used for network construction using Cytoscape 3.7.2 (Figure 5).

Gene ontology and KEGG pathway analyses of mRNAs were used to explored the potential roles of ceRNAs. GO enrichment

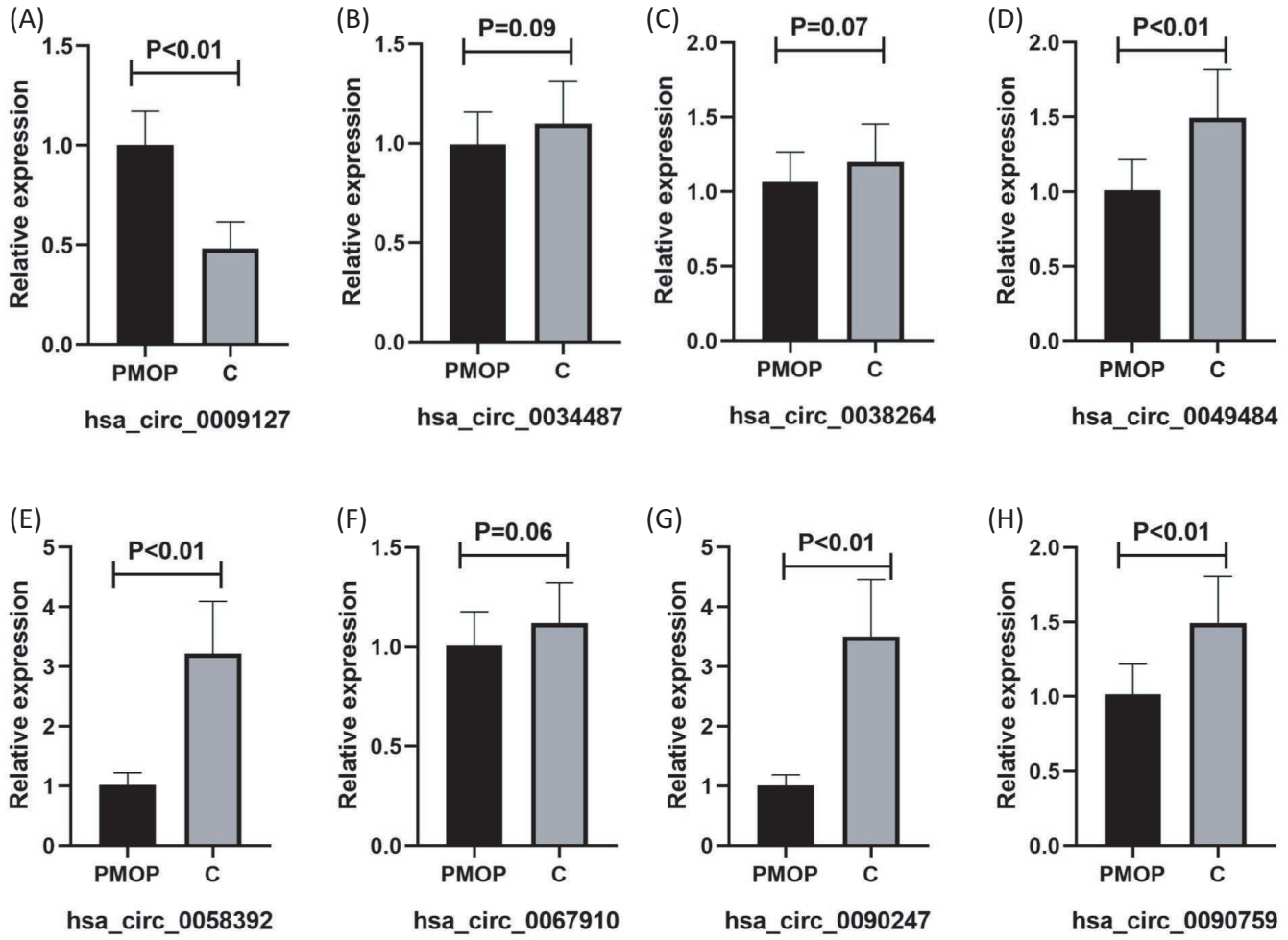

FIGURE 4 RT-qPCR validation of target circRNA in the PMOP group vs control group. Expression levels of (A) hsa_circ_0009127, (B) hsa_circ_0034487, (C) hsa_circ_0038264, (D) hsa_circ_0049484, (E) hsa_circ_0058392, (F) hsa_circ_0067910, (G) hsa_circ_0090247, and (H) hsa_circ_0090759

analyses showed the distribution of the number of differential genes on GO term enriched under biological process (BPs), cellular components (CCs), and molecular functions (MFs) (Figure 6A). Analysis showed that GO:0045335 (phagocytic vesicle), GO:0043931 (ossification involved in bone maturation), GO:0060346 (bone trabecula formation), GO:0045778 (positive regulation of ossification), and GO:0001649 (osteoblast differentiation) were enriched (Additional file 2). The most significant KEGG terms were involved in the regulation of autophagy, transcriptional dysregulation in cancers, PI3K-Akt signaling, and FoxO signaling (Figure 6B). Affected transcripts were associated with cellular pathways related to MAPK and Hippo signaling, which are involved in osteogenic differentiation.

4 | DISCUSSION

The application of BMSCs for bone tissue repair and rejuvenation has received significant attention in recent years.[5,24,25] Several studies report that paracrine actions constitute the primary mechanism by which BMSCs exert therapeutic effects.[26,27] Exosomes are paracrine factors, which mediate intercellular communication and are important effectors of BMSCs.[28,29] Several studies have explored the differential expression patterns of non-coding RNAs (ncRNAs) in blood mononuclear and lymphocyte cells from PMOP patients, including lncRNAs, mRNAs, circRNAs, and miRNAs.[30,31] Some differentially expressed lncRNAs play important roles in osteogenic differentiation and bone regeneration.[32,33] In addition, differentially expressed circRNAs including circRNA_007438 and circRNA_005108,[34] circRNA BANP, and circRNA ITCH play modulatory roles during osteoclastogenesis and osteogenic differentiation.[35] However, the differential expression profiles of circRNA in PMOP BMSCs exosomes have not been explored and their regulatory mechanism on osteogenic, and adipogenic differentiation of BMSCs is not fully known.

In the current study, BMSCs-derived exosomes were obtained from PMOP patients and control groups, and circRNA expression

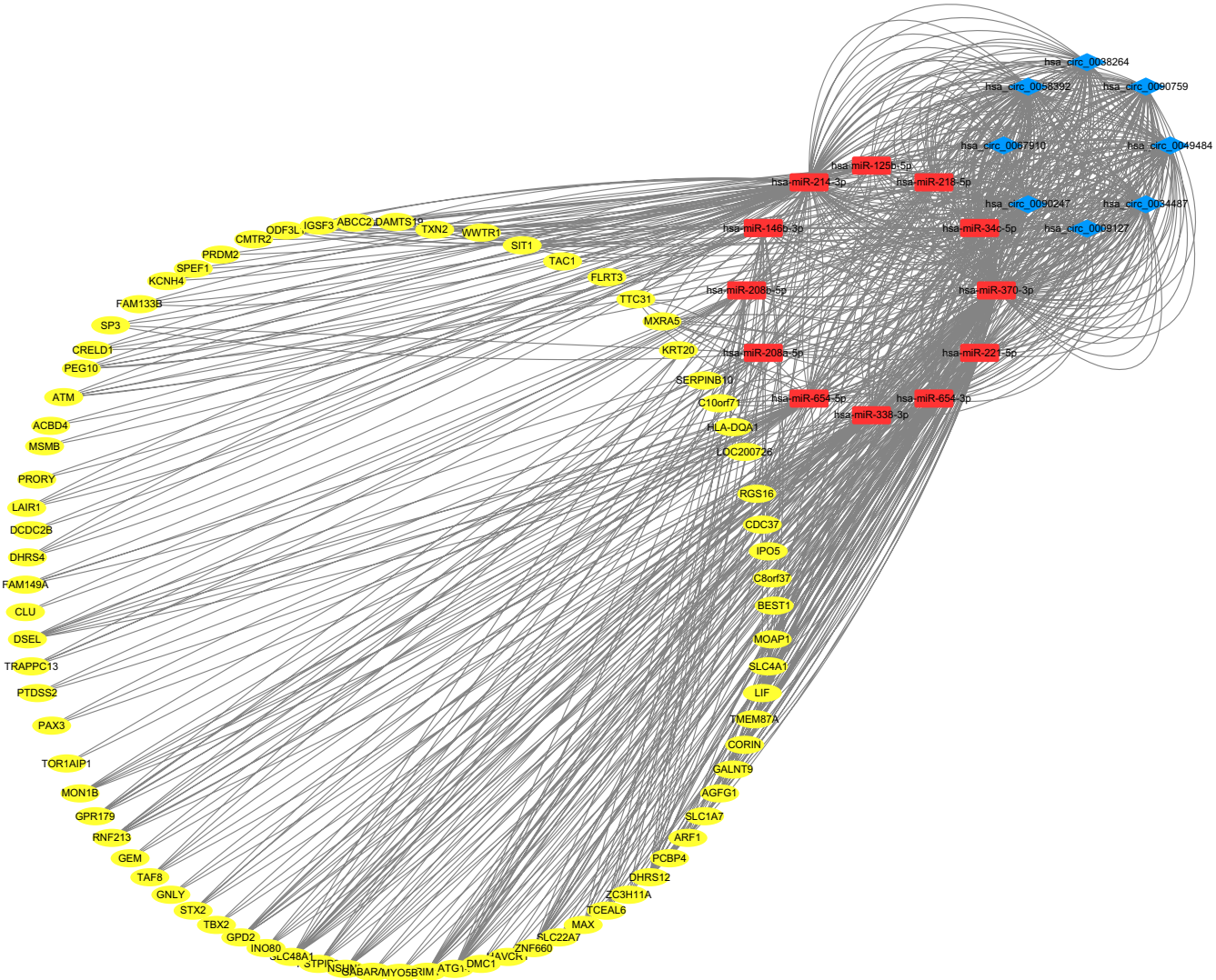

FIGURE 5 The circRNA-miRNA-mRNA network. Blue diamonds represent circRNAs. Red rectangles represent miRNAs. Yellow ovals represent mRNAs

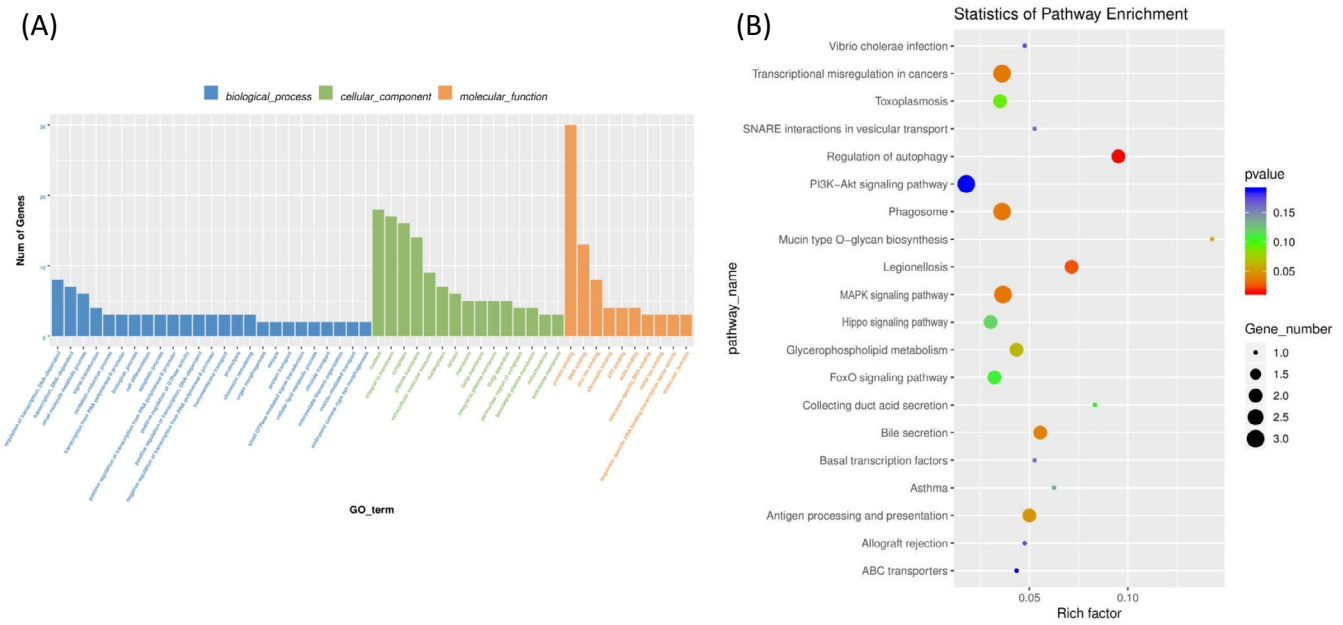

FIGURE 6 ceRNA network GO and KEGG enrichment analysis

profiles and those controls were evaluated. A total of 516 circRNAs were differentially expressed in exosomes from PMOP BMSCs and control BMSCs exosomes (|FC|≥1.5, $p = <0.05$). Out of the 516 differentially expressed circRNAs, 237 were upregulated, whereas 279 were downregulated. RT-qPCR analysis of 5 differentially expressed circRNAs (hsa_circ_0009127, hsa_circ_0090759, hsa_circ_0058392, hsa_circ_0090247, and hsa_circ_0049484) was used to verify microarray results. The biological roles of the 5 circRNAs have not been reported before. The function of these circRNAs was not explored in this study, as the main aim was to explore the potential mechanisms of competing endogenous RNA.

Hsa_circ_0058392 may modulate osteogenic differentiation through ceRNA interactions. MiRanda and TargetScan analyses showed that Hsa_circ_0058392 interacts with hsa-miR-214. Osteoclast-derived exosomal miR-214 enhances osteoclastogenesis by modulating PI3K/Akt signaling by targeting phosphatase and tensin homolog.[36] Analysis showed that Hsa_circ_0058392 interacts with hsa-miR-221, which negatively regulates osteogenic differentiation by repressing RUNX2, and were downregulated in exosomes from BMSCs.[37] Hsa-miR-148a-3p, hsa-miR-338-3p, hsa-miR-124-3p, hsa-miR-155, hsa-miR-221, and hsa-miR-214 were recently reported to play important roles in osteogenesis[38,39]; therefore, the findings of the current study provide information on the regulatory mechanism. The findings show the role of hsa_circ_0009127, hsa_circ_0090759, hsa_circ_0058392, hsa_circ_0090247, and hsa_circ_0049484. However, circRNA-related ceRNA networks in PMOP are complex. The finding of the present study provided a basis for further exploring circRNA-related ceRNA networks in PMOP.

Gene ontology and KEGG pathway analyses were outperformed to elucidate the roles of mRNAs in circRNA-linked ceRNA networks. GO analyses showed that factors in this network may be involved in PMOP pathogenesis, including phagocytic vesicle (GO: 0045335), ossification involved in bone maturation (GO: 0043931), and bone trabecula formation (GO: 0060346). Tissue regeneration initiated by MSC occurs in a paracrine manner, and the observed enrichment of exosomes and phagocytic vesicles (GO: 0045335) indicates the central role of this process in regeneration.[40] KEGG pathway analysis showed that these differentially expressed circRNAs may be implicated in the regulation of autophagy, PI3K-Akt signaling, FoxO signaling, and MAPK signaling. Previous studies report that autophagy regulates osteoblast differentiation.[41,42] Additionally, autophagy counteracts oxidative stress elevation during aging; thus, autophagy plays an important roles in PMOP.[43] PI3K-Akt signaling promotes osteoblast proliferation, differentiation, and osteogenesis, thus inhibiting osteoporosis.[44] Osteogenic differentiation of BMSCs into osteoblasts is a well-controlled process modulated by several factors such as Runx2, β-catenin, Osx, and alkaline phosphatase.[45] Recent studies report that interactions between FoxO members and differentiation modulatory factors lead to bidirectional modulation of osteogenic differentiation in MSCs.[46] MAPK signal pathway is the core regulatory pathway triggered by hypoxia, and hypoxia affects the cell cycle, proliferation, apoptosis, migration, and differentiation of MSCs.[47,48] Although PMOP regulation by genes identified in the current study was not explored, the study of exosomes from PMOP patients' BMSCs provides a basis for the understanding of PMOP pathogenesis.

In the current study, the expression of circRNAs in PMOP patients' BMSCs exosomes and normal control BMSCs exosomes was explored. A total of 5 differentially expressed circRNAs (hsa_circ_0009127, hsa_circ_0090759, hsa_circ_0058392, hsa_circ_0090247, and hsa_circ_0049484), which can be used as potential PMOP biomarkers and potential therapeutic targets for the treatment of PMOP were identified. A total of 516 differentially expressed circRNAs were identified. Most of these circRNAs are implicated in pathological processes linked to the regulation of autophagy, PI3K-Akt signaling, FoxO signaling, and MAPK signaling.

Although the study was limited to functional analysis and did not perform functional verification, these findings provide information on the role of circRNAs in the etiology and pathogenesis of PMOP.

CONFLICTS OF INTEREST

Miao Fu, liping Fang, Xi Xiang, Xijing Fan, Junqi Wu, and Jinhua Wang declare that they have no conflict of interest.

AUTHOR CONTRIBUTIONS

Miao Fu, Xi Xiang, and Jinhua Wang designed the research. Xijing Fan and Jinhua Wang conducted the acquisition of data. Miao Fu and liping Fang provided technical and material supports.; Junqi Wu, Miao Fu, and Xi Xiang analyzed data and wrote the article. Junqi Wu conducted a critical revision of the manuscript.

DATA AVAILABILITY STATEMENT

Data used in this study cannot be shared for both legal and ethical reasons. The data include participant information and can only be used for the purpose stated in the license granted, scientific research on society by the license applicant, and can, therefore, not be shared to the public. However, data can be obtained from the corresponding author upon reasonable request.

ORCID

Junqi Wu https://orcid.org/0000-0002-4134-8797
Jinhua Wang https://orcid.org/0000-0002-6042-1822

REFERENCES

1. Black DM, Rosen CJ. Clinical practice. Postmenopausal osteoporosis. *N Engl Med*. 2016;374(3):254-262.
2. Heidenreich R, Lee R, Shil AB. Osteoporotic fractures in postmenopausal women. *J Am Geriatr Soc*. 2017;65(3):e76.
3. Cai XP, Zhao Q, et al. Potential diagnostic value of PD-1 in peripheral blood mononuclear cells of postmenopausal osteoporosis patients. *J Clin Lab Anal*. 2020;34(6):e23223.
4. Fang H, Zhang H, Wang Z, Zhou Z, Li Y, Lu L. Systemic immune-inflammation index acts as a novel diagnostic biomarker for postmenopausal osteoporosis and could predict the risk of osteoporotic fracture. *J Clin Lab Anal*. 2020;34(1):e23016.
5. Griffin M, Iqbal SA, Bayat A. Exploring the application of mesenchymal stem cells in bone repair and regeneration. *J Bone Joint Surg Br*. 2011;93(4):427-434.
6. Antebi B, Pelled G, Gazit D. Stem cell therapy for osteoporosis. *Curr Osteoporos Rep*. 2014;12(1):41-47.
7. Liu S, Liu D, Chen C, et al. MSC transplantation improves osteopenia via epigenetic regulation of notch signaling in lupus. *Cell Metab*. 2015;22(4):606-618.
8. Yuan FL, Wu QY, Miao ZN, et al. Osteoclast-derived extracellular vesicles: novel regulators of osteoclastogenesis and osteoclast-osteoblasts communication in bone remodeling. *Front Physiol*. 2018;9:628.
9. Kourembanas S. Exosomes: vehicles of intercellular signaling, biomarkers, and vectors of cell therapy. *Annu Rev Physiol*. 2015;77:13-27.
10. Toh WS, Lai RC, Hui JHP, Lim SK. MSC exosome as a cell-free MSC therapy for cartilage regeneration: implications for osteoarthritis treatment. *Semin Cell Dev Biol*. 2017;67:56-64.
11. Cui Y, Luan J, Li H, Zhou X, Han J. Exosomes derived from mineralizing osteoblasts promote ST2 cell osteogenic differentiation by alteration of microRNA expression. *FEBS Lett*. 2016;590(1):185-192.
12. Zhang L, Jiao G, Ren S, et al. Exosomes from bone marrow mesenchymal stem cells enhance fracture healing through the promotion of osteogenesis and angiogenesis in a rat model of nonunion. *Stem Cell Res Ther*. 2020;11(1):38.
13. Cosenza S, Ruiz M, Toupet K, Jorgensen C, Noël D. Mesenchymal stem cells derived exosomes and microparticles protect cartilage and bone from degradation in osteoarthritis. *Sci Rep*. 2017;7(1):16214.
14. Mao G, Zhang Z, Hu S, et al. Exosomes derived from miR-92a-3p-overexpressing human mesenchymal stem cells enhance chondrogenesis and suppress cartilage degradation via targeting WNT5A. *Stem Cell Res Ther*. 2018;9(1):247.
15. Qi X, Zhang J, Yuan H, et al. Exosomes secreted by human-induced pluripotent stem cell-derived mesenchymal stem cells repair critical-sized bone defects through enhanced angiogenesis and osteogenesis in osteoporotic rats. *Int J Biol Sci*. 2016;12(7):836-849.
16. Zeckser J, Wolff M, Tucker J, Goodwin J. Multipotent mesenchymal stem cell treatment for discogenic low back pain and disc degeneration. *Stem Cells Int*. 2016;2016:3908389.
17. Li Y, Zheng Q, Bao C, et al. Circular RNA is enriched and stable in exosomes: a promising biomarker for cancer diagnosis. *Cell Res*. 2015;25(8):981-984.
18. Li Z, Ruan Y, Zhang H, Shen Y, Li T, Xiao B. Tumor-suppressive circular RNAs: Mechanisms underlying their suppression of tumor occurrence and use as therapeutic targets. *Cancer Sci*. 2019;110:3630-3638.
19. Li X, Yang L, Chen LL. The biogenesis, functions, and challenges of circular RNAs. *Mol Cell*. 2018;71:428-442.
20. Liu J, Liu T, Wang X, He A. Circles reshaping the RNA world: from waste to treasure. *Mol Cancer*. 2017;16:58.
21. Shen S, Wu Y, Chen J, et al. CircSERPINE2 protects against osteoarthritis by targeting miR-1271 and ETS-related gene. *Ann Rheum Dis*. 2019;78(6):826-836.
22. Cherubini A, Barilani M, Rossi RL, et al. FOXP1 circular RNA sustains mesenchymal stem cell identity via microRNA inhibition. *Nucleic Acids Res*. 2019;47(10):5325-5340.
23. Parkhomchuk D, Borodina T, Amstislavskiy V, et al. Transcriptome analysis by strand-specific sequencing of complementary DNA. *Nucleic Acids Res*. 2009;37(18):e123.
24. Liu B, Yang F, Wei X, et al. An exploratory study of articular cartilage and subchondral bone reconstruction with bone marrow mesenchymal stem cells combined with porous tantalum/Bio-Gide collagen membrane in osteonecrosis of the femoral head. *Mater Sci Eng C Mater Biol Appl*. 2019;99:1123-1132.
25. Fan Y, Hanai JI, Le PT, et al. Parathyroid hormone directs bone marrow mesenchymal cell fate. *Cell Metab*. 2017;25(3):661-672.
26. Abbaszadeh H, Ghorbani F, Derakhshani M, Movassaghpour A, Yousefi M. Human umbilical cord mesenchymal stem cell-derived extracellular vesicles: a novel therapeutic paradigm. *J Cell Physiol*. 2020;235(2):706-717.
27. Lai RC, Yeo RW, Lim SK. Mesenchymal stem cell exosomes. *Semin Cell Dev Biol*. 2015;40:82-88.
28. Vonk LA, van Dooremalen SFJ, Liv N, et al. Mesenchymal stromal/stem cell-derived extracellular vesicles promote human cartilage regeneration in vitro. *Theranostics*. 2018;8(4):906-920.
29. Zhu LP, Tian T, Wang JY, et al. Hypoxia-elicited mesenchymal stem cell-derived exosomes facilitates cardiac repair through miR-125b-mediated prevention of cell death in myocardial infarction. *Theranostics*. 2018;8(22):6163-6177.
30. Jin D, Wu X, Yu H, et al. Systematic analysis of lncRNAs, mRNAs, circRNAs and miRNAs in patients with postmenopausal osteoporosis. *Am J Transl Res*. 2018;10(5):1498-1510.

31. Tong X, Gu PC, Xu SZ, Lin XJ. Long non-coding RNA-DANCR in human circulating monocytes: a potential biomarker associated with postmenopausal osteoporosis. *Biosci Biotechnol Biochem*. 2015;79(5):732-737.
32. Wang Q, Li Y, Zhang Y, et al. LncRNA MEG3 inhibited osteogenic differentiation of bone marrow mesenchymal stem cells from postmenopausal osteoporosis by targeting miR133a-3p. *Biomed Pharmacother*. 2017;89:1178-1186.
33. Peng W, Zhu SX, Wang J, Chen LL, Weng JQ, Chen SL. Lnc-NTF3-5 promotes osteogenic differentiation of maxillary sinus membrane stem cells via sponging miR-93-3p. *Clin Implant Dent Relat Res*. 2017;20(2):110-121.
34. Dou C, Cao Z, Yang B, et al. Changing expression profiles of lncRNAs, mRNAs, circRNAs and miRNAs during osteoclastogenesis. *Sci Rep*. 2016;6:21499.
35. Gu X, Li M, Jin Y, Liu D, Wei F. Identification and integrated analysis of differentially expressed lncRNAs and circRNAs reveal the potential ceRNA networks during PDLSC osteogenic differentiation. *BMC Genet*. 2017;18(1):100.
36. Zhao C, Sun W, Zhang P, et al. miR-214 promotes osteoclastogenesis by targeting Pten/PI3k/Akt pathway. *RNA Biol*. 2015;12(3):343-353.
37. Xu JF, Yang GH, Pan XH, et al. Altered microRNA expression profile in exosomes during osteogenic differentiation of human bone marrow-derived mesenchymal stem cells. *PLoS One*. 2014;9(12):e114627.
38. Xie Y, Chen Y, Zhang L, Ge W, Tang P. The roles of bone-derived exosomes and exosomal microRNAs in regulating bone remodelling. *J Cell Mol Med*. 2017;21(5):1033-1041.
39. Yao X, Wei W, Wang X, Chenglin L, Björklund M, Ouyang H. Stem cell derived exosomes: microRNA therapy for age-related musculoskeletal disorders. *Biomaterials*. 2019;224:119492.
40. Billing AM, Ben Hamidane H, Dib SS, et al. Comprehensive transcriptomic and proteomic characterization of human mesenchymal stem cells reveals source specific cellular markers. *Sci Rep*. 2016;6:21507.
41. Hu Z, Chen B, Zhao Q. Hedgehog signaling regulates osteoblast differentiation in zebrafish larvae through modulation of autophagy. *Biol Open*. 2019;8(5):bio040840.
42. Nollet M, Santucci-Darmanin S, Breuil V, et al. Autophagy in osteoblasts is involved in mineralization and bone homeostasis. *Autophagy*. 2014;10(11):1965-1977.
43. Filaire E, Toumi H. Reactive oxygen species and exercise on bone metabolism: friend or enemy? *Joint Bone Spine*. 2012;79(4):341-346.
44. Xi JC, Zang HY, Guo LX, et al. The PI3K/AKT cell signaling pathway is involved in regulation of osteoporosis. *J Recept Signal Transduct Res*. 2015;35(6):640-645.
45. An J, Yang H, Zhang Q, et al. Natural products for treatment of osteoporosis: the effects and mechanisms on promoting osteoblast-mediated bone formation. *Life Sci*. 2016;147:46-58.
46. Chen D, Gong Y, Xu L, Zhou M, Li J, Song J. Bidirectional regulation of osteogenic differentiation by the FOXO subfamily of Forkhead transcription factors in mammalian MSCs. *Cell Prolif*. 2019;52(2):e12540.
47. Sun X, Jin Y, Liang Q, et al. Altered expression of circular RNAs in human placental chorionic plate-derived mesenchymal stem cells pretreated with hypoxia. *J Clin Lab Anal*. 2019;33(3):e22825.
48. Li L, Jaiswal PK, Makhoul G, et al. Hypoxia modulates cell migration and proliferation in placenta-derived mesenchymal stem cells. *J Thorac Cardiovasc Surg*. 2017;154:543-552.

SUPPORTING INFORMATION

Additional supporting information may be found in the online version of the article at the publisher's website.

How to cite this article: Fu M, Fang L, Xiang X, Fan X, Wu J, Wang J. Microarray analysis of circRNAs sequencing profile in exosomes derived from bone marrow mesenchymal stem cells in postmenopausal osteoporosis patients. *J Clin Lab Anal*. 2022;36:e23916. https://doi.org/10.1002/jcla.23916